Ozone episodes in Catalonia during the summer of 2019. A meteorological and photochemical modeling analysis.

Author: Clara Jaen Flo
Supervisor: Mireia Udina Sistach, mudina@ub.edu
*Facultat de Física, Universitat de Barcelona, Diagonal 645, 08028 Barcelona, Spain.**

Abstract: During the summer of 2019 unusual exceedances of ozone concentration affected Catalan territory. In the present work, a deep study of two ozone episodes is performed, focusing on the flow circulation and potential sources. Episode A occurred on June 28 and June 29 and Episode B on July 23. Both episodes are characterized by synoptic anticyclonic conditions, surface temperatures over the 95th percentile and high ozone values recorded inland due to precursors advection (NO_x and VOCs) mainly from Barcelona Metropolitan Area (AMB). The analysis of measured time series and the comparison with ARAMIS modeled concentrations showed that advection on June 28 and July 23 made its way through the eastern Barcelona valley and through the western one on June 29. Modeled-observation comparison maps reflect the general tendency of the model to overestimate modeled peak areas, to slightly underestimate in the rest of the territory and to rise ozone values few hours before they are measured. Moreover, a trajectory analysis confirmed recirculation between June 28 and June 29 and concentration weighted trajectory maps determined the pathways linking the receptors with the AMB as the main potential sources for the cities of Vic and Manresa. Finally, NO_2 measured in Barcelona was found to have influence in urban and rural ozone concentrations.

I. Introduction

Tropospheric ozone is a secondary atmospheric pollutant with strong oxidizing properties. Measured ozone concentrations depend on local formation and background but also in long-range and regional transport. Ozone formation is strongly affected by the presence of sunlight and precursors such as NO_x (sum of NO and NO_2), CH_4, CO and volatile organic compounds (VOCs). It is known to have damaging effects on human health, vegetation and materials. Ozone formation processes are usually initiated by the photolyisis of NO_2 by interaction with solar radiation and its destruction may be inhibited by hydroxyl (OH) or peroxy radicals (HO_2) in presence of CO, CH_4 or other organic compounds.

Part of the ozone chemistry is still unknown and formation sensibility to both main precursors (NO_x and VOCs) is under investigation. *Sillman and He* (2002) evaluated chemical factors that regulate two different regimes: NO_x-limited and VOCs-limited. Under high VOCs/NO_x ratios ozone is more sensitive on NO_x, increasing its concentration if NO_x does . This NO_x-sensitive regime is more common in suburban and rural areas situated downwind from emission sources. On the other hand, under low VOCs/NO_x ratios, increasing NO_x may reduce O_3. This VOCs-limited regime takes place in urban areas which can actually register higher ozone values on non-working days due to road traffic reduction. This is known as "weekend effect" (*Adame et al.* (2014)).

Nonlinear temperature and humidity relations with ozone production have been described by several studies. Generally, increasing temperature and decreasing relative humidity lead to an increase of tropospheric ozone levels (*Camalier et al.* (2007)). In the expected climate change scenario, global warming will increase ozone production in polluted areas whereas ozone background levels are expected to be reduced due to higher water vapour concentrations. *Pusede et al.* (2015) described five chemical variables involved in ozone-temperature relationship including the organic reactivity to hydroxyl radical and NO_x lifetime. Consequently, as a result of this dependence on solar radiation and temperature, ozone concentrations are highly variable along the year and day, usually being maximum at midday on summer days.

Over western Mediterranean seaside areas, O_3 dynamics are influenced by coastal recirculations driven by sea breezes. Night seaward wind flows can create pollutant layers at different elevations over the sea. These layers sink during day-time leaving ozone reservoirs at low levels that can be advected to the land when breezes onset. This mechanism can exist during several consecutive days depending on the synoptic meteorological contitions. In this scenario, high insulation conditions enhance photochemical transformations into oxidants of the accumulated pollutants (*Millán et al.* (1997)). Other mechanism observed is O_3 fumigation. It occurs during the morning growth of the Boundary Layer which introduces previous days O_3 from the residual layer (stored at height during night-time) and contributes to rising surface ozone concentrations (*Querol et al.* (2017)).

Ozone episodes occur when ground-level concentrations exceed threshold values set by legislation. In Catalonia, air quality standards are sometimes exceeded and tropospheric ozone is usually under special surveillance. The objective of this study is to characterize two ozone episodes that took place in Catalonia during the summer of 2019. A deep study of the influencing meteorological factors, the areas affected, the consequences and the capacity to forecast the events will be performed.

* Electronic address: cljaenfl7@alumnes.ub.edu

II. Methodology

A. Study area

This study is focused in Catalonia, an autonomous community in northeastern Spain characterized by complex topography. The relief of Catalonia presents three main morph-structural units: the Pyrenees, the highest mountainous formation in the north, a double system of mountain chains parallel to the coast called the Catalan Mediterranean System, and the Central Depression located between the previous.

Most of the population and industrial areas are located on the coast, mainly in the capital, Barcelona. The high industrial activity and road and shipping transport emissions in the Barcelona Metropolitan Area (AMB) compose the most important source of NO_x and VOCs in the Catalan territory. Several valleys crossing the coastal Catalan ranges favour pollutant transport from AMB to inland cities like Vic (across Besòs-Congost rivers valley) or Manresa (across Llobregat river valley). Hence, anthropogenic emissions of NO_x and VOCs combined with biogenic VOCs and high insulation may cause severe ozone episodes in inland settled areas.

B. Local Legislation and measurament network

Catalan territory is divided into 4 *provinces* and further subdivided into 41 *comarques*. In order to evaluate and monitor air quality, the territory is divided in 15 Air Quality Zones according to their emission and dispersion conditions. This distribution allows to optimize ground level measurement stations for the *Xarxa de Vigilància i Previsió de la Contaminació Atmosfèrica* (XVPCA). This public network is responsible for pollutants measurements in the autonomous community and it is managed by the Catalan Territory and Sustainability Department. Nowadays, XVPCA operates with 75 automatic stations classified according to local emissions (background, industrial or traffic) and soil use (rural, suburban or urban). Ozone is measured in 49 of these stations. In compliance with Directive 2008/50/EC adopted in *Reial Decret* 102/2011 the institution monitors ozone levels. It defines and sets Air Quality Goals (AQG) which determine the level of each pollutant that, when exceeded, implies legal actions to reduce human health impact. In case of ozone, the Air Quality Goals concerning this work are the following:

- **IT** (Information Threshold): Hourly-mean values can not exceed 180 $\mu g/m^3$.
- **AT** (Alert Threshold): Hourly-mean values can not exceed 240 $\mu g/m^3$.

Pollutants measured in XVPCA stations are just the ones regulated in the European directives including the ozone precursor NO_2. However, there is no control on most of VOCs.

C. Modelling

Pollutant species forecasting (O_3 and NO_2) is modeled with the high resolution air quality model ARAMIS (A Regional Air Quality Modelling Integrated System) developed by the Mesoscale and Microscale Atmospheric Modelling and Research group (MAiR) from the University of Barcelona (*Soler et al.* (2015)). It integrates meteorological, emission and photochemical data from three Eulerian models: the Weather Research and Forecasting model (WRF-ARW), version 3.5, the High Resolution Emission Model (HIREM) and the Community Multiscale Air Quality Modelling System (CMAQ), version 5.1, respectively. Three nested domains are configured, with horizontal resolutions of 27 km (D1), 9 km (D2) and 3 km (D3) using one way nesting. In this study we use the D3 domain that covers the area of interest. For each day, simulations are run for 72h, taking the first 24 h as spin-up time to minimise the effects of initial conditions.

Air parcels trajectories have been calculated with the Hybrid Single-Particle Lagrangian Integrated Trajectory (HYSPLIT) model developed by the National Oceanic and Atmospheric Administrations (NOAA) (*Stein et al.* (2015)). In this study, WRF-ARW meteorological data in specific gridded format for HYSPLIT has been used to analyze simple forward and backward trajectories affecting XVPCA stations measurements.

Furthermore, a potential source analysis has been done for two representative receptor stations located in Llobregat (Manresa) and Besòs-Congost (Vic) pollutants pathways. To achieve this, the concentration-weighted trajectory (CWT) method developed by *Hsu et al.* (2003) has been used. 10 hours backward trajectories ending in target stations during June, July and August of 2019 at high concentration hours have been calculated using HYSPLIT model. The high concentration hours have been chosen by those when June, July and August average was over 80 $\mu g/m^3$. In the case of Vic, from 9 UTC to 19 UTC and from 10 UTC to 17 UTC for Manresa. The division of the study area in grid cells allowed to assign each cell a weighted ozone concentration value by averaging ozone concentrations measured in the receptor associated with each trajectory with endpoints falling in the cell as follows:

$$C_{ij} = \frac{\sum_{l=1}^{M} C_l \tau_{ijl}}{\sum_{l=1}^{M} \tau_{ijl}}$$

where C_{ij} is the average weighted concentration in the i, j grid cell, C_l the measured ozone concentration in the receptor, τ_{ijl} the number of trajectory endpoints in the i, j grid cell associated with C_l and M the number of samples that have trajectory endpoints in the i, j grid cell. To minimize the uncertainty of CWT values calculated with few endpoints, an arbitrary weight function ($W_{i,j}$) proposed by *Zeng and Hopke* (1989) has been multiplied to each CWT value depending on the number of endpoints falling in the cell ($n_{i,j}$) in relation to the average.

$W_{i,j}$ is defined as:

$$W_{i,j} = \begin{cases} 1,00 & if \quad n_{i,j} > 3,0Avg \\ 0,70 & if \quad Avg < n_{i,j} \leq 3,0Avg \\ 0,42 & if \quad 0,5Avg < n_{i,j} \leq Avg \\ 0,17 & if \quad 0 < n_{i,j} \leq 0,5Avg \end{cases}$$

III. Results

Results are organized in two parts. Firstly, a general view of ozone situation in Catalonia over the years and the particularities of 2019. And secondly, an specific study of two ozone episodes which occurred in 2019.

A. Background

The year 2019 had several days with abnormally high hourly ozone values with 115 hours of Information Threshold Exceedances (ITEs) and 7 hours of Alert Threshold Exceedances (ATEs). These high values are very unusual for the last decade even in an area like Catalonia with problematic ozone concentrations. The normalized Alert Threshold incidences [1] from 1991 to 2019 (Fig. 1) are high between 1991 and 2003 and inexistent from 2007 to 2018 probably due to more emission restrictions set by European and local legislation in the beginning of the twenty-first century. The normalized Information Threshold incidences show a great variability along the years but also present higher values during the first monitoring years. Understanding the meteorology, chemical and transport processes involved in these high ozone concentration episodes is necessary to take action for decreasing human health impact caused by these events. In the present work, we will try to understand the factors influencing the rise in ATEs on 2019.

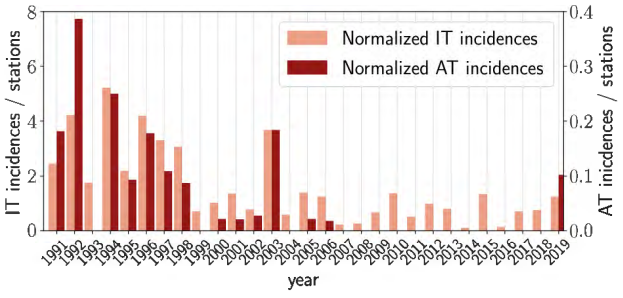

Figure 1: Normalized AT and IT incidences for each year since the beginning of monitoring to 2019.

Under usual summer meteorological conditions, the Azores High located in the western side of the Iberian peninsula and a ridge at height extending into southern Europe combined with mesoscale phenomena lead to a complex circulation in the area. A diurnal cycle in wind direction (southerlies during solar hours and northerlies at night) can be observed and previous studies demonstrated these surface winds can produce recirculations of pollutants (*Gangoiti et al.* (2001)). This synoptic pattern can coexist with a high pressure located in center Europe. In this situation, Catalonia can be affected by easterly advection of pollutants due to marine surface flows. In general, with low pressure gradients under anticyclonic driven situations, flow is controlled by thermal effects so sea breezes have a great development and long-range advection of air masses is not remarkable.

Prevailing anticyclonic situations lead to dry summers with high temperatures over the Iberian peninsula. Fig. 2 shows the 2 m temperature reanalysis for June, July and August of 2019 compared with data since 1979. Hourly data was obtained from ECMWF ERA5 reanalysis covering the studied region both from 850 hPa (see Appendix Fig. A.1) and surface heights and averaged in day and space. During the summer of 2019, 95th percentile temperature was exceeded 15 days at surface levels and 11 days at 850 hPa. Abnormally high temperatures were obtained from June 26 to June 30 and from July 22 to July 25. For both periods, 6 day-long heat waves were declared by local authorities reaching maximum heat wave temperatures[2] of 38.8 °C and 36.8 °C, respectively. Ozone episodes studied in the present work took place during those periods. This is consistent with the correlation between high temperature and ozone formation previously explained. In fact, 104 ITEs (out of 115 for all summer) occurred in days when the surface reanalysed temperature exceeded the 95th percentile.

B. 2019 Episodes

In this study, we will focus on the two most intense ozone episodes that took place during the summer of 2019. The first one, Episode A, was two-day long episode from June 28 to June 29 and Episode B occurred in July 23. Simultaneous characterization will be performed to analyze the causes, consequences, similarities and differences between both episodes. Their main characteristics are summarized in Table I including the exceptional number of exceedances during the episodes which disrupt the trends of previous years (*Massagué et al.* (2019)). Also, a schematic map is shown in Fig. 3 which includes main breeze components, affected areas for the studied days and also the most important cities influenced during both episodes.

Regarding the synoptic meteorology, both episodes are characterized by surface anticyclones situated over the Azores and British Isles or central Europe, a thermal low in central Iberia and a high pressure ridge at 500

[1] An incidence is a group of consecutive hours with threshold exceedances during the ozone surveillance campaign.

[2] Highest daily average of the maximum temperatures measured at the stations affected by the heat wave.

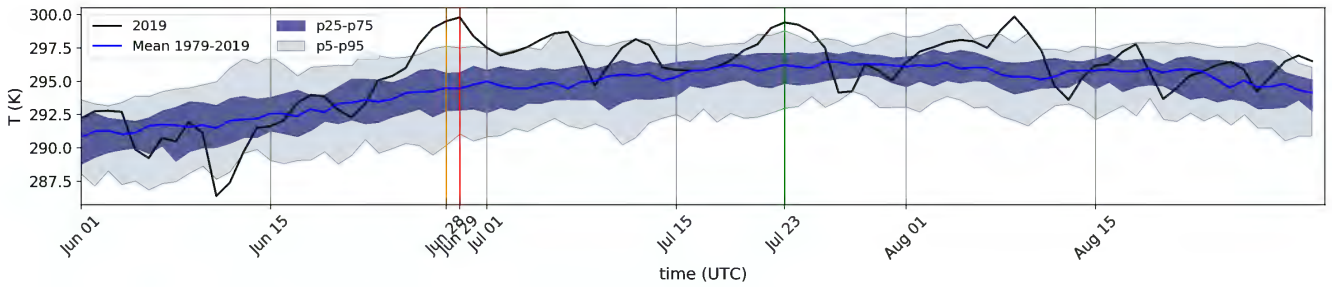

Figure 2: Daily average ERA 5 reanalysis of 2 m temperature in Catalan territory for June, July and August from 1979 to 2019. Dark blue and light grey shaded areas show values from 25th to 75th and from 5th to 95th percentiles, respectively. Coloured (orange, red and green) lines correspond to the analyzed episode days (section B).

hPa extended to most of the Mediterranean basin. For the specific days, midday reanalysis of June 28 displays a relative high over Gulf of Biscay which may induce northerlies in the north of Catalonia. For June 29, a cyclonic rotation was placed south of Gulf of Lion leading to strong northerlies in the northern coast of Catalonia. On the other hand, July 23 surface flows are essentially southerlies along the day.

	Episode A		**Episode B**
Day	June 28	June 29	July 23
ITEs (n° of hours)	20 h	49 h	10 h
n° of stations with ITEs	8	17	6
ATEs (n° of hours)	4 h	1 h	2 h
n° of stations with ATEs	3	1	2
Reanalyzed 2 m temperature over the 95th percentile (Days)	26-30 June		22-25 July
Maximum heat wave tempererature	38.8 °C		36.8 °C

Table I: Summary of the main episodes characteristics.

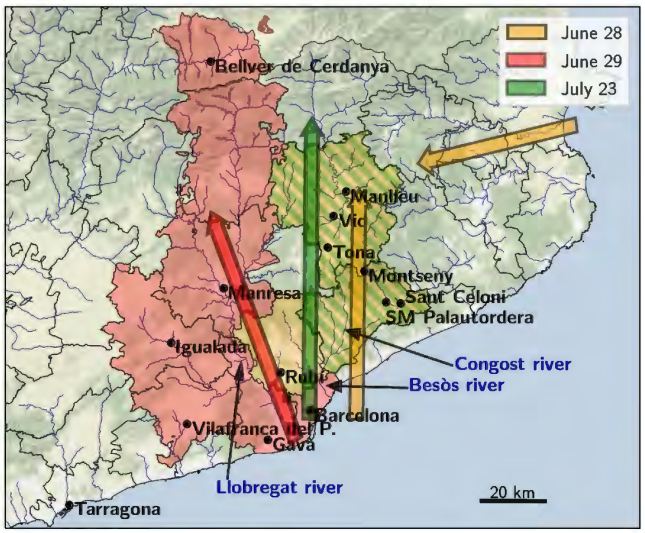

Figure 3: Schematic representation of main sea breeze contributions and affected regions for both episodes.

In the north-east part of Catalonia sea breezes have more westward direction due to coast orientation and flow has both advection and breeze contributions. The different intensity of both northward and westward sea breeze components will determine the location of the convergence area, therefore, which will be the dominant pollutant advection pathway. For the studied episodes, surface winds show that wind convergence over Catalan territory is located further west for June 29 than for June 28 and July 23 (see Fig. 3).

1. *Station measurements*

In Episode A, the IT was exceeded in 25 XVPCA stations and in 4 XVPCA stations for Episode B. In order to better understand the analyzed ozone time-series, only those from stations with ozone hourly values over 200 $\mu g/m^3$ are shown in Fig. 4. In all cases, ATEs happened between 12 and 14 UTC when solar radiation is more intense and temperatures are higher. For both episodes the peak values evolution gives information about surface flow motion. On June 28 (Fig. 4a), the earliest peaks were registered in Rubí and Sant Celoni, stations relatively near to the high emission source area of Barcelona. As time passed peak values were observed in stations farther from the coastline: in Montseny, Tona, Vic and Manlleu at 14, 14, 15 and 16 UTC respectively, as diurnal breeze penetrates inland through north-eastern valleys of Barcelona (Besòs-Congost pathway).

For June 29, ozone time series of stations located in *Barcelonès comarca* (Fig. 4b) are represented separately from those located in the rest of Catalonia. Concentration in Observatory Fabra was higher than in other stations in Barcelona most part of the day, and particularly high at late afternoon. This station is located at 415 m above sea level which indicates an accumulation of pollutants at high altitudes in the coast. For non-*Barcelonès*

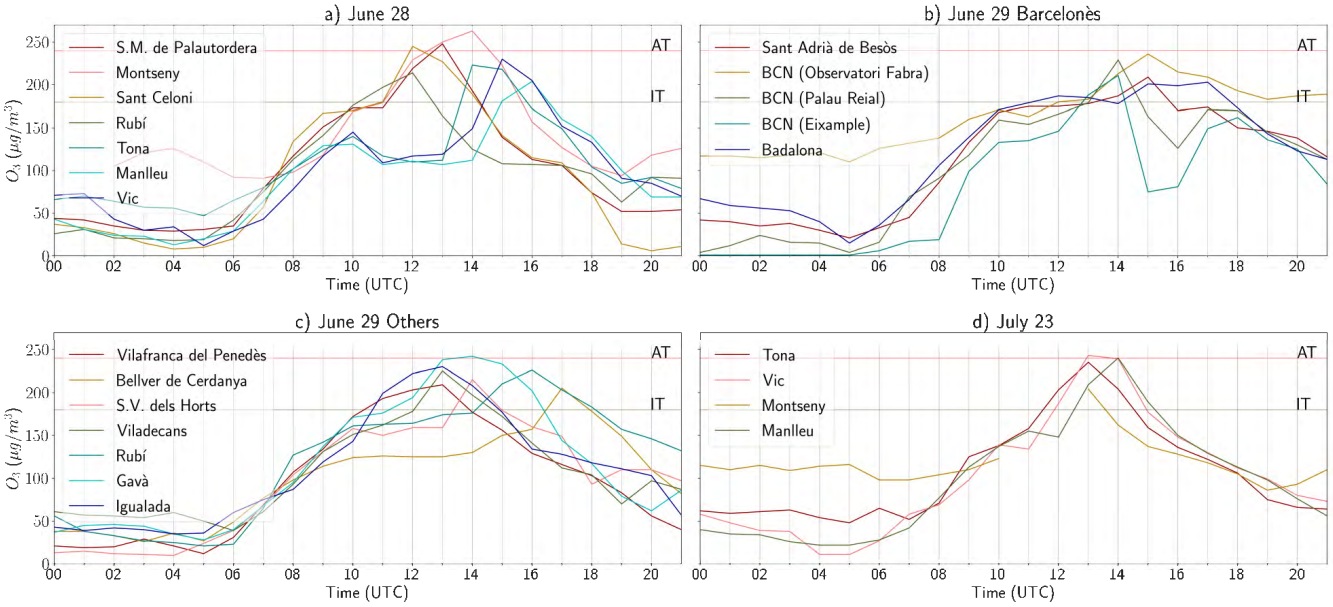

Figure 4: Time series of O_3 concentration in stations with some hourly value over 200 μg/m^3 during both episodes.

stations, peak evolution in Fig. 4c shows that sea breeze advected pollutants through western Barcelona Valleys (Llobregat pathway) during that day and high values were recorded even in Bellver de Cerdanya, located in the south part of the Pyrenees, about 100 km away from Barcelona (see Fig. 3). As mentioned above, surface wind convergence determines the dominant pollutant advection pathway affecting different areas both days.

Ozone concentration time series for Episode B are represented in Fig. 4d. Flow evolution follows a similar pattern than in June 28 but fewer stations were affected by high ozone concentrations. As it was seen for the previous episode, maximum values evolve inland with time. Firstly, the ozone peak is observed in Tona, and afterwards in Vic and Manlleu. Technical problems altered measures in Montseny and no values were recorded from 10 to 13 UTC which may be higher than the later measured. Both episode days with exceedances in this station show high night concentrations compared with the other stations. Montseny Massif is part of the catalan pre-coastal range and the XVPCA station is placed at 693 m of altitude compared with 145 m or 460 m of Sant Celoni and Manlleu, respectively. Therefore, Montseny may be measuring background ozone concentrations remaining in high altitudes due to sea breeze recirculation (*Soler et al.* (2011)), similar to what is observed in Episode A during night-time in Observatory Fabra.

2. Modelling

Time series of modeled and observational ozone values of representative stations are compared in Fig. 5. It

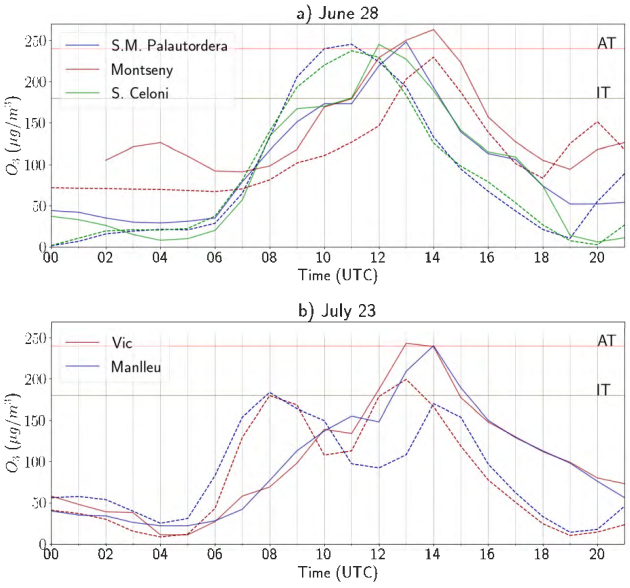

Figure 5: Modeled (dashed) and measured (solid) time series from representative stations for two episode days.

is shown that for June 28 (Fig. 5a) ARAMIS predicted almost correctly the maximum values reached in Santa Maria de Palautordera and Sant Celoni but before they was actually measured. This tendency of the model to estimate values earlier than they occurred is seen in many occasions. In addition, model estimated high values over a larger period of time. However, in the case of Montseny station, both peaks coincide in time but measured time series is always higher except at late afternoon. On the

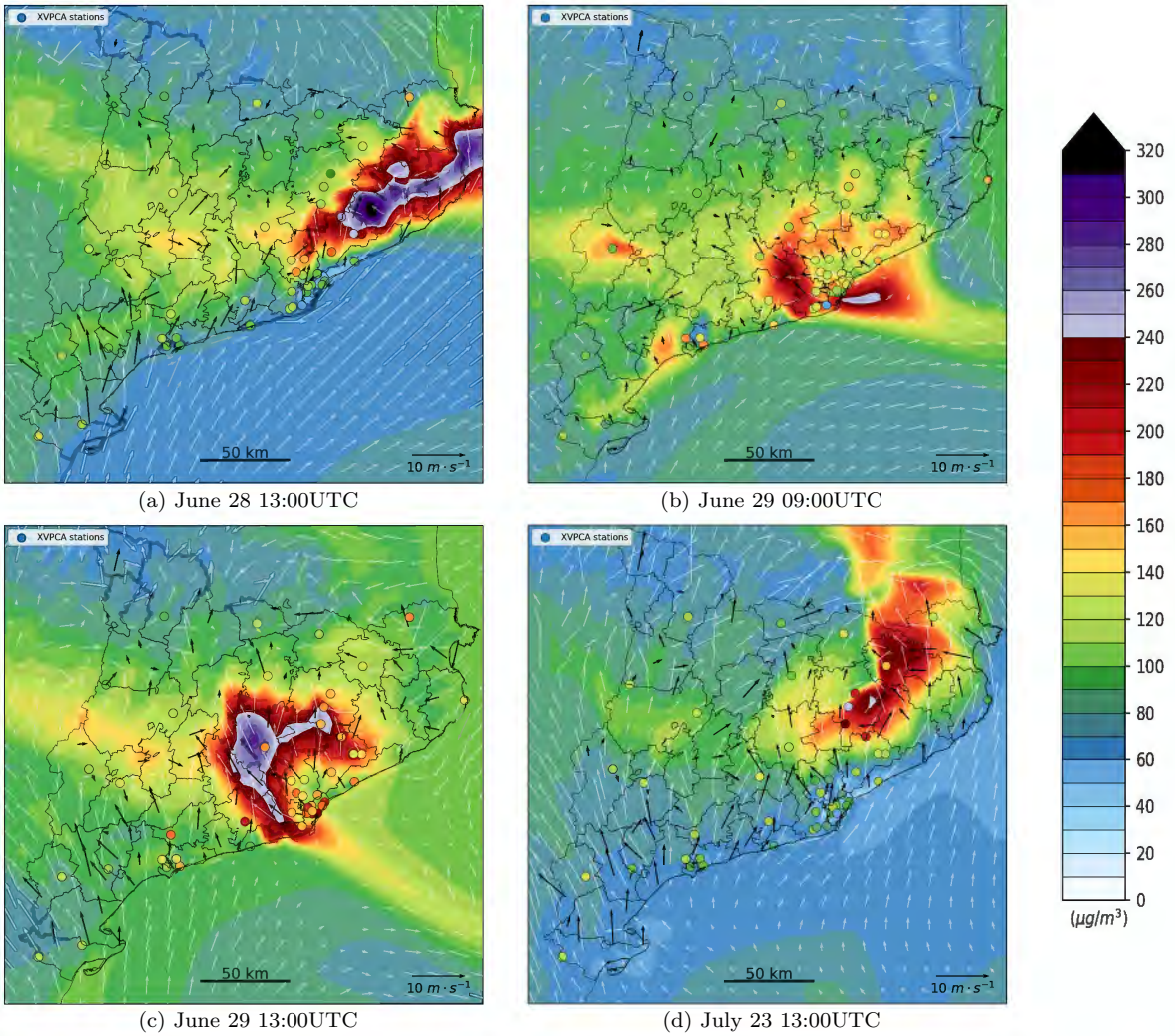

(a) June 28 13:00UTC (b) June 29 09:00UTC

(c) June 29 13:00UTC (d) July 23 13:00UTC

Figure 6: Modeled and observed ozone concentrations in Catalonia for 4 different times. Shaded contour plot shows modeled values while coloured dots correspond to XVPCA station measurements. WRF-ARW wind direction and module at 10 m are represented by white arrows and 10 m wind measured by Catalan Meteorological Service stations are represented by black arrows. Complementary maps are shown in Appendix Fig. A.4.

other hand, the simulation approximately describes the previously explained elevated night-time ozone concentrations in Montseny.

For June 23 (Fig. 5b), the model simulation reproduces the near-midday peaks in time, slightly underestimating the ozone concentrations in Vic and Manlleu. During morning hours, ARAMIS forecasts values reaching the IT, a peak that is not seen in the observational values. This feature is repeated in several simulated episodes and is rarely measured.

The simulation results allow us to compare forecasts in several measuring stations around Catalonia and to explore spatial ozone concentrations and wind patterns in areas where there are no measurements. The most representatives of the comparative maps from both episodes are shown in Fig. 6. They include the ozone concentration value forecasted by the model (shaded color) and measured by the XVPCA stations (colored dots). They also include the simulated wind field (grey arrows) and the wind vector measured by stations from the Catalan Meteorological Service (Meteocat) (black arrows). In order to highlight the most affected area, ozone values over AT have been represented in violet tonalities.

As diurnal heat got stronger and breezes onsetted during June 28, model peak was displaced from north Barcelona to the north-east part of Catalonia (Fig. 6a) through Besòs-Congost pathway. As previously explained, some stations, Sant Celoni, Santa Maria and Montseny revealed ATE, that were pretty well estimated by ARAMIS. Moreover, the model estimates ozone concentrations reaching very high values (about 300 $\mu g/m^3$) further in the north-east area (comarques such as *La Selva* and *Baix Empordà*) where there are no measurement stations and unfortunately, these values can not be

verified. In this region, we can also see the easterly flow component entering inland through Gulf of Roses which can also contribute to rise O_3 concentrations. During the following hours, peak values were displaced northward to Vic plain reaching the last maximum in Manlleu at 16 UTC. Meteocat winds confirm advection of AMB pollution to inland stations and the convergence of easterly and southerly flows at onshore regions. As a response of this convergence, the anabatic winds and the northerlies blowing in the Pyrenees, pollutants were transported upwards and may be distributed towards the sea by breeze aloft. Along night-time, wind weakly blown among north components as a result of coupled effect of downslope night winds and breezes. This airflow may therefore transport ozone to the coast.

Morning of June 29 (Fig. 6b), reveals an ozone plume in front of Barcelona coast consistent with the aforementioned pollutant recirculation. Ozone and its precursors can be trapped in stacked layers formed along the coast and come back to land the next day, what is called ozone fumigation. Hence, ATE measured in Gavà at 14 UTC may be explained by means of ozone formation via precursors reaction with the morning solar radiation over the sea and the latter transport inland combined with ozone recirculation and ozone fumigation from residual layer. In addition, the main wind component at the port of Barcelona was found to be westward, towards Gavà and Llobregat valley, following an unusual direction. This implied not only advection from sea air layers but also from all emissions from port of Barcelona industrial activity. However, the origin of this peak is not clearly defined because it took place later than other peaks located farther from the coast and it lasted during 3 hours, so it could also be caused by local emissions.

Along June 29 (Fig. 6c), model peak was displaced north-west of Barcelona following the Llobregat river pathway and reached the Central Depression. In this case, measured peaks were observed latter than the modeled ones, feature seen before, and most of them were much lower than the estimated value. Although maximum values in Llobregat valley evolved onshore with time following the sea breeze front, concentrations in AMB remained constantly high until late afternoon. These values far exceeded the predicted ones at the coast. Yet, model forecast correctly ozone concentration in Bellver de Cerdanya at 17 UTC, sea breeze had a great extent capable of carry pollutants to the Pyrenees. Otherwise, even though ARAMIS forecast ATE in Vic surroundings there were not even ITEs there.

Difference in pollutants trajectory both days was mainly because of strong Tramuntana (northerlies in the north-east coasts) blowing at morning hours of June 29 compared to southerlies observed there for June 28. During June 28, south-westerlies of the sea flow penetrated inland with sea breezes, thus, southerlies are observed all around the territory. In this scenario, flow motion moves generally through eastern Barcelona Besòs-Congost pathway. However, during June 29 early hours, northerlies blew along the north coast turning to north-easterlies with time. In this case, convergence with south-westerlies blowing along the south coast occurs in front of Barcelona and advects recirculated and newer pollutants through Llobregat pathway (Fig. 6c).

Episode B corresponds to July 23. The general circulation and flow advection is similar to the first part of episode A (June 28). The main difference is that southerlies were stronger for July 23 and there were no northerlies blowing in the Pyrenees. Hence, winds all along the coast had strong south components and air masses were transported north by flow motion in almost all territory (Fig. 6d). Even so, there were also easterlies in north-east of Catalonia due to breeze circulation perpendicular to the coast. Ozone high concentrations affected mainly Vic surroundings and the maximum was clearly displaced inland with time. ARAMIS model also predicted high values before they were measured and situated the maximum displaced slightly to the east of Vic. In this case, pollution also reached high values in the pre-Pyrenean station of Pardines at 16 UTC, located north from Manlleu, consistent with stronger northward fluxes during all day. Predicted ozone was lower than measured in the rest of the territory for most of daily hours and some wind components from AMB advected to Manresa and relative high concentrations were also measured there.

3. Simple trajectory analysis

Backward trajectories for the most representative station computed with HYSPLIT model using WRF-ARW meteorological simulations from the ARAMIS system are shown in Fig. 7. In all cases, stations which measured ATE present trajectories passing though AMB. For June 28, air from Barcelona took between 3 and 4 hours to arrive to the affected stations, which means that NO_2 from morning traffic rush hours reach the stations at midday when sunlight is stronger. As it can be observed in Tona's trajectory, high values in Vic plain can also be attributed to precursors transport from Barcelona. However, trajectories in this location may not be very well estimated for peak hours. HYSPLIT uses WRF-ARW wind to generate trajectories, therefore if the real wind is not reproduced correctly neither will the trajectories. Previously explained hourly comparison allowed to see how southerly flow breezed inland and converged with easterly winds. However, wind observations advertised that northward breeze front penetrated further than model predicted and so did advection from AMB. For this particular moment, it was observed that modeled wind turned from easterlies to southerlies around Vic area latter than the measured. Hence, to better estimate the trajectories ending at Tona, Vic and Manlleu they were started one hour after the measured peak took place. Despite this, trajectories in the northern stations still came from the east. Consequently of this difference in wind direction between model and observations, ARAMIS un-

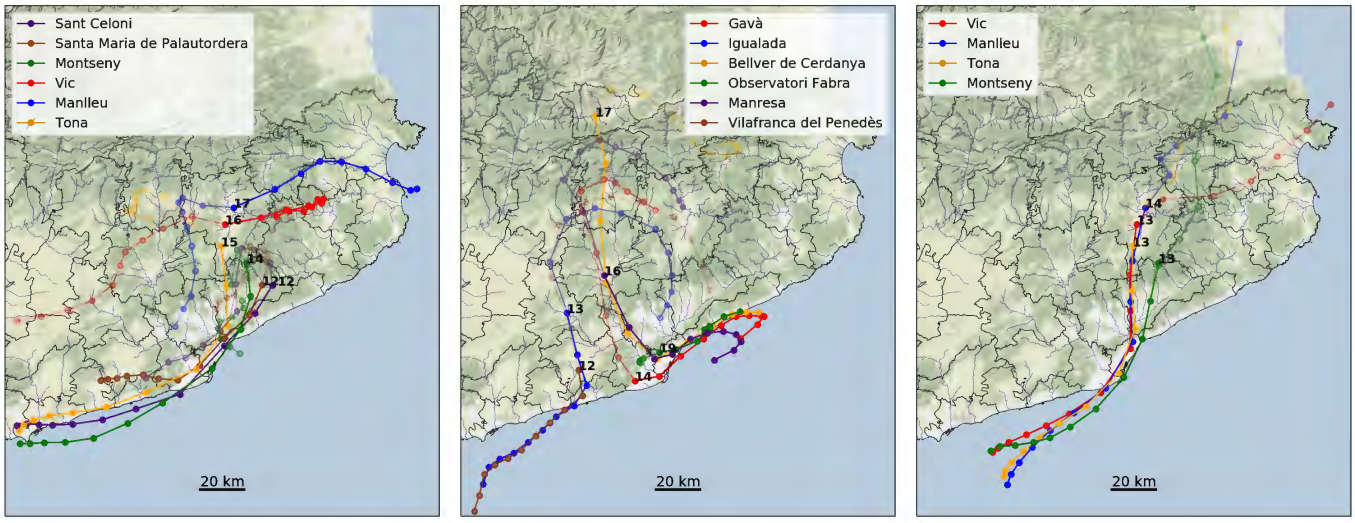

(a) June 28 (b) June 29 (c) July 23

Figure 7: Trajectories from most the representative stations for both episodes. Full coloured and semitransparent lines correspond to backward and forward trajectories, respectively. The number next to the station correspond to the UTC hour when both simulations started.

derestimated values in Vic plain. On the other hand, the observed westward advection could also bring pollutants from southern France or Italy (regional transport) and contribute to high ozone values measured and modeled in the north-east coast.

Regarding the forward trajectories for June 28, a clear recirculation to the sea is observed in many stations. Trajectory in Montseny, the highest station of the ones represented, shows that the air mass is over the sea in front of Barcelona 10 hours later, consistent with the sea-breeze recirculation and storage in layers on the coast, pattern previously explained.

For June 29, two different kind of backward trajectories were described (Fig. 7b). The ones ending in Igualada and Vilafranca come from the sea in front of Tarragona, a highly industrialized area in the south coast of Catalonia. Pollutants may be advected over the sea from industries the day before, but given the concentrations measured then, the main contribution should be the mixing after convergence with flow coming from Barcelona coast. This air mixing is blocked at shoreline by Garraf Massif but may result inland. On the other hand, air flow affecting Llobregat valley came, as expected, from above the sea in front of Barcelona. It passed through the capital driven by easterlies and headed north guided by Llobregat pathway. It took 6 hours to the air flow to go from Barcelona to Bellver de Cerdanya. For Observatory Fabra backward trajectory, which was started at 19 UTC, air parcel is barely displaced remaining in Barcelona surroundings for most of the hours. This indicates that high Barcelona ozone concentrations along the afternoon may have the same origin as the advected inland and that local topography prevent part of the recirculated pollutants to disperse, rising concentrations in the capital. For this day, forward trajectories also indicate some kind of recirculation that can affect high values also measured for June 30.

During Episode B, trajectories also come from the city of Barcelona and they also took between 3 and 4 hours to reach the measurement points. In contrast to June 28, in Episode B southerly breezes are stronger and advection is produced further north. Moreover, easterlies are weaker and vertical transport is not strong enough to recirculate pollutants. Strong southerlies of bigger scales are the reason why recirculation is not observed, as it can be seen in forward trajectories heading north. As it was seen for June episode, this plays a key role on high concentration episodes as an important recirculation after a high episode day may lead to ITEs in many areas the next day.

4. Potential source analysis

In order to determine the impact of the trajectories analyzed for both episodes a potential source analysis for all 2019 summer trajectories (June, July and August) have been done for Vic (representative of Besòs-Congost pathway affecting area) and Manresa (representative of Llobregat valley). The concentration-weighted trajectory (CWT) maps have been done for Vic and Manresa and are shown in Fig. 8. In them, points with higher weighted concentrations (closer to yellow) represent the areas where the air masses passing through them gave higher ozone concentrations when reaching the receptor station. These points can be interpreted as potential

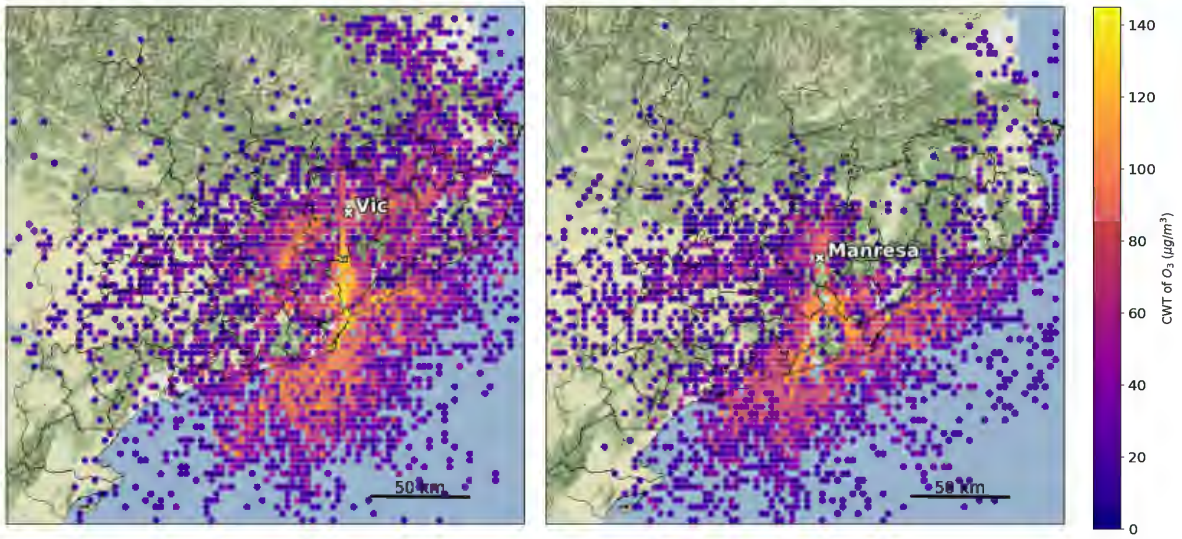

(a) Vic, trajectories from 9 UTC to 19 UTC.

(b) Manresa, trajectories from 10 UTC to 17 UTC.

Figure 8: CWT maps for summer trajectories ending in Vic and Manresa at hours with June, July and August average over 80 μg O_3/m^3.

sources thanks to the weight function applied. However, it is necessary to remember that all endpoints of each trajectory have the same concentration associated and we cannot know where the pollution sources were located. Hence, these maps allow to determine the wind direction which is more likely to give high ozone concentrations in the receptor.

In the case of Vic (Fig. 8a), higher CWT values are located at the coast of Barcelona and along the straight line linking the capital with Vic, coherent with the behaviour observed for June 28 and July 23. Strong southerly breezes developed in summer use to rise ozone in Vic surroundings. Another potential source areas are located east and west from the station following a very busy traffic road know as *Transversal Arterial Road* (C-25), which may be the main NO_x source for air masses coming from both directions. This road links both stations (Vic and Manresa) and we can see that trajectories passing through Manresa give high ozone concentrations in Vic. On the other hand, high CWT values north from the station may be associated with northerly breezes in late afternoon which transport ozone seaward. However, the hourly CWT analysis show that during earlier hours the trajectories are mainly from the north, east and west and the south ones are associated with latter hours when breezes reach the station (see Appendix Fig. A.2). Hence, north high CWT cells may result from morning northerlies.

For Manresa (Fig. 8b), trajectories passing through Barcelona have less importance than for Vic, and the main potential sources are Llobregat valley and west from Garraf Massif according to both kind of trajectories previously described for June 29. In addition, contributions from the west part of the C-25 and north of station are also observed. Nevertheless, just few trajectories come with the synoptic flow or breezes from the east part of Catalonia. This indicates that this flow rarely penetrates further than Vic plain and this area is not a potential source region for Manresa station.

For both stations, relatively high CWT values are found over the sea. In case of recirculation and accumulation in stratified layers there, advection with sea breezes also have contribution to rise concentrations inland.

In addition, this analysis confirms that the trajectories studied for episodes A and B usually give high ozone concentrations in Llobregat and Besòs-Congost pathways, even though there is not always exceedences.

5. NO_2

Comparative maps of modeled and measured concentrations were also done for NO_2 so a comparison between both pollutants can give information about the chemistry involved (see Appendix Fig. A.3). Concentrations above 230 $\mu g/m^3$ (hourly value) of NO_2 were measured in Barcelona at morning hours of June 28 exceeding by far model expected values. Consequently, and consistent with NO_x-limited regime previously explained, suburban stations downwind from Barcelona emissions record high O_3 concentrations due to NO_x advection. However, O_3 values measured in Barcelona stations were low. The next day, saturday 29 of June, NO_2 in AMB at early hours were lower than the day before and was better predicted by ARAMIS model. As expected in an urban VOCs-limited regime, ozone in Barcelona was very high. Hence, this indicates that weekend effect have also a contribution in this episode. On the other hand, July 23 was a thursday of holiday period and NO_2 values were low. In spite of that, ozone in Barcelona is also low and higher values are recorded inland. These differences suggest that main contribution to high ozone values in Barcelona for June 29 is recirculation rather than emitted NO_2 influence.

IV. Conclusions

In this work, two high ozone episodes were described for the summer of 2019. Episode A took place between the 28th and 29th of June (4 ATEs and 1 ATE, respectively) and Episode B the 23rd of July (1 ATE). Both were characterized by high temperatures (over the 95th percentile), driven by the sea breeze circulation in areas where the main ozone contribution was the advection of NO_x from AMB and its mixture with VOCs emitted by local sources. All combined with high temperatures and strong solar radiation enhancing ozone formation.

According to XVPCA measurements, the inland evolution of ozone peaks was through eastern Barcelona valleys (Besòs-Congost pathway) for June 28 and July 23 and through western valleys (Llobregat pathway) for June 29. These ozone peaks evolution is reproduced by the ARAMIS modeled O_3 values. The general tendency of ARAMIS forecasting is to overestimate the areas where the peak of O_3 concentrations occur and slightly underestimate O_3 concentrations in the rest of the territory. Another usual characteristic in modeled ozone is to increase O_3 concentrations few hours before they are measured. In June 28, modeling results suggest concentrations over 300 $\mu g/m^3$ in the north-east of the territory, which cannot be verified by observations but remarks the necessity of monitoring ozone concentrations in the air quality zone of *Comarques de Girona*. Additionally, modeled flows confirmed accumulation over the sea and recirculation in Episode A which may be the major reason for the big number of exceedances measured on June 29.

Trajectory analysis confirms the NO_x advection from AMB as a main cause of high ozone concentrations inland as almost all trajectories analyzed passed through this area several hours before reaching the stations with exceedances. Forward trajectories also support the hypothesis of recirculation and accumulation of pollutants over the sea for June 28 and less intense for June 29 whilst no recirculation is observed for June 23.

Potential sources for Vic and Manresa reinforce the fact that described trajectories usually rise ozone in both stations during summer seasons. The major potential source for Vic is Barcelona and the straight line linking both cities while for Manresa is Llobregat valley.

Concerning the relation with NO_2, behaviours of NO_x-limited and VOCs-limited regimes are observed for June 28 in onshore regions and for June 29 in Barcelona, respectively, whilst for June 23 the relation is not clear.

Acknowledgments

I would like to express my appreciation to my TFM advisor, Mireia Udina, for all her patience and valuable advice during all my stay in the research group. Also to all people in the department who helped me at some point of my work. Thanks to Territory and Sustainability Department and Meteocat for the data. And finally, special thanks to my family and friends for their support.

References

Adame, J. A., M. Á. Hernández-Ceballos, M. Sorribas, A. Lozano, and B. A. De la Morena, Weekend-weekday effect assessment for o3, nox, co and pm10 in andalusia, spain (2003–2008), *Aerosol and Air Quality Research*, *14*(7), 1862–1874, 2014.

Camalier, L., W. Cox, and P. Dolwick, The effects of meteorology on ozone in urban areas and their use in assessing ozone trends, *Atmospheric Environment*, *41*(33), 7127–7137, 2007.

Gangoiti, G., M. M. Millán, R. Salvador, and E. Mantilla, Long-range transport and re-circulation of pollutants in the western mediterranean during the project regional cycles of air pollution in the west-central mediterranean area, *Atmospheric Environment*, *35*(36), 6267–6276, 2001.

Hsu, Y.-K., T. M. Holsen, and P. K. Hopke, Comparison of hybrid receptor models to locate pcb sources in chicago, *Atmospheric Environment*, *37*(4), 545–562, 2003.

Massagué, J., C. Carnerero, M. Escudero, J. M. Baldasano, A. Alastuey, and X. Querol, 2005-2017 ozone trends and potential benefits of local measures as deduced from air quality measurements in the north of the barcelona metropolitan area, *Atmospheric Chemistry and Physics*, *19*(11), 7445–7465, 2019.

Millán, M., R. Salvador, E. Mantilla, and G. Kallos, Photooxidant dynamics in the mediterranean basin in summer: Results from european research projects, *Journal of Geophysical Research: Atmospheres*, *102*(D7), 8811–8823, 1997.

Pusede, S. E., A. L. Steiner, and R. C. Cohen, Temperature and recent trends in the chemistry of continental surface ozone, *Chemical reviews*, *115*(10), 3898–3918, 2015.

Querol, X., et al., Phenomenology of high-ozone episodes in ne spain, *Atmospheric Chemistry and Physics*, *17*(4), 2817–2838, 2017.

Sillman, S., and D. He, Some theoretical results concerning o3-nox-voc chemistry and nox-voc indicators, *Journal of Geophysical Research: Atmospheres*, *107*(D22), ACH–26, 2002.

Soler, M., R. Arasa, M. Merino, M. Olid, and S. Ortega, Modelling local sea-breeze flow and associated dispersion patterns over a coastal area in north-east spain: a case study, *Boundary-layer meteorology*, *140*(1), 37–56, 2011.

Soler, M. R., P. Gamez, and M. Olid, Aramis a regional air quality model for air pollution management: evaluation and validation, *Física de la Tierra*, *27*, 113–138, 2015.

Stein, A., R. R. Draxler, G. D. Rolph, B. J. Stunder, M. Cohen, and F. Ngan, Noaa's hysplit atmospheric transport and dispersion modeling system, *Bulletin of the American Meteorological Society*, *96*(12), 2059–2077, 2015.

Zeng, Y., and P. Hopke, A study of the sources of acid precipitation in ontario, canada, *Atmospheric Environment*, *23*(7), 1499–1509, 1989.

A. Complementary Figures.

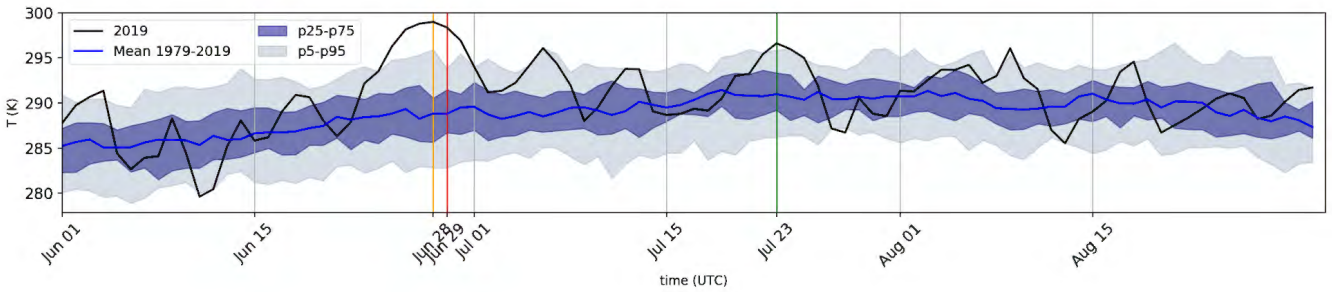

Figure A.1: Daily average ERA 5 reanalysis temperature at 850 hPa in Catalan territory for June, July and August from 1979 to 2019. Dark blue and light grey shaded areas show values from 25th to 75th and from 5th to 95th percentiles, respectively. Coloured (orange, red and green) lines correspond to the analyzed episode days (section B).

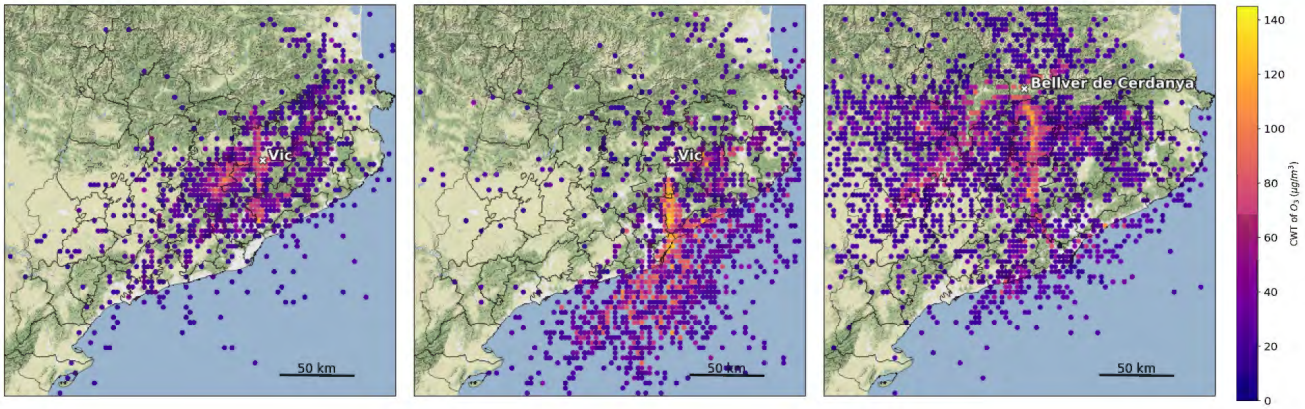

(a) Vic from 9 UTC to 11 UTC. (b) Vic from 17 UTC to 19 UTC (c) Bellver from 9 UTC to 19 UTC

Figure A.2: CWT maps for summer trajectories ending in Vic at different hours, at morning hours (a), at afternoon hours (b) and ending in Bellver at hours with June, July and August average over 80 μg O_3/m^3 (c).

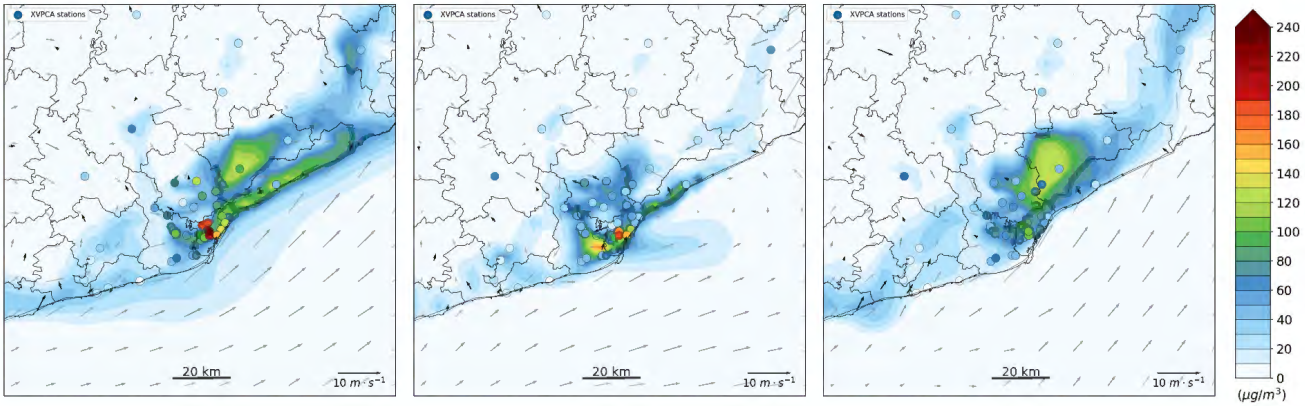

(a) June 28 08:00 UTC (b) June 29 08:00 UTC (c) July 23 08:00 UTC

Figure A.3: Modeled (ARAMIS) and observed NO_2 in Barcelona surroundings for each day of the studied episodes at 8 UTC.

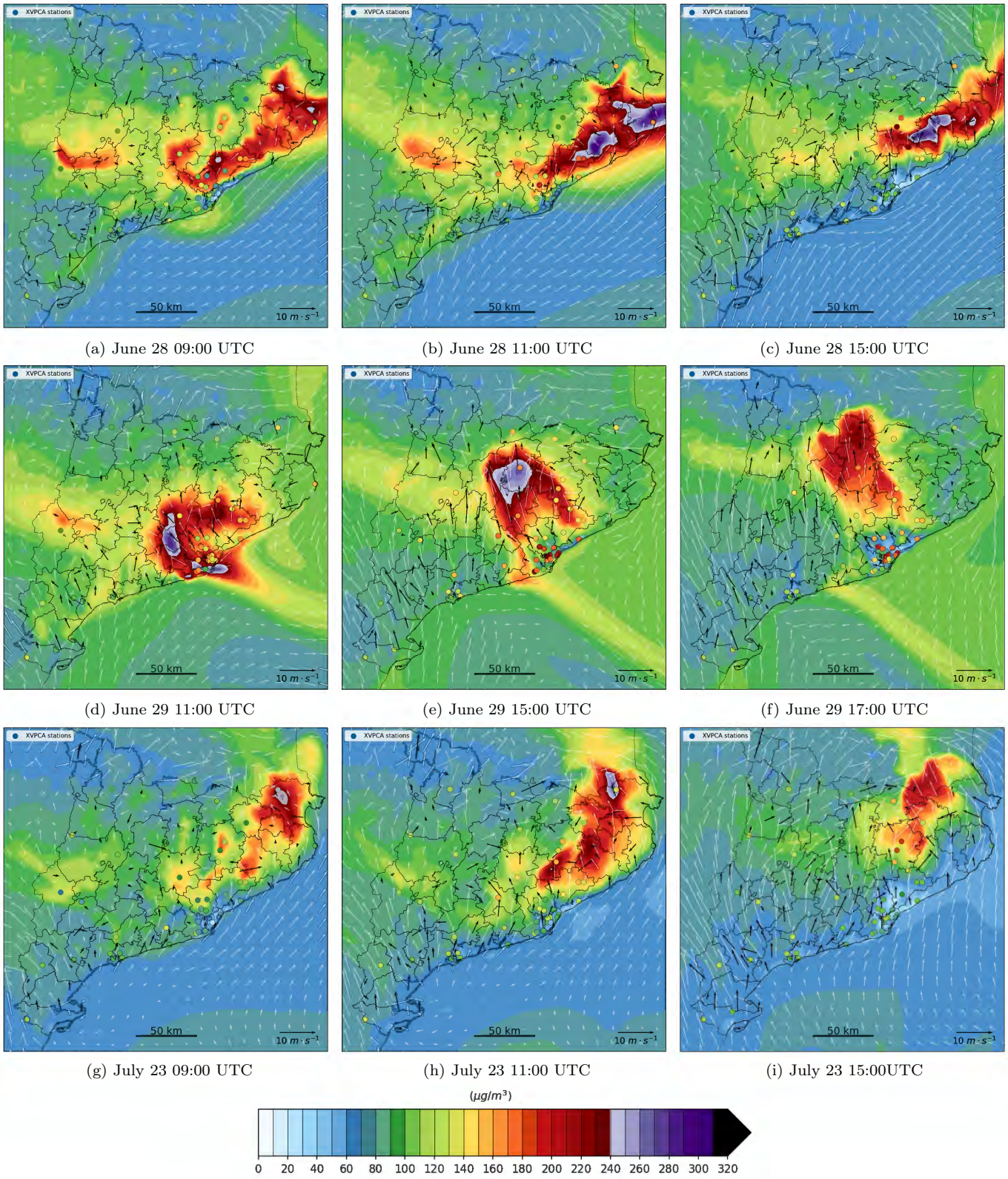

(a) June 28 09:00 UTC (b) June 28 11:00 UTC (c) June 28 15:00 UTC

(d) June 29 11:00 UTC (e) June 29 15:00 UTC (f) June 29 17:00 UTC

(g) July 23 09:00 UTC (h) July 23 11:00 UTC (i) July 23 15:00UTC

Figure A.4: Modeled (ARAMIS) and observed ozone in Catalonia for different times to complete information of the episodes shown in Fig. 6. Contour plot shows model values while rounded marks show station measurements at its location. WRF-ARW wind direction and module at 10 m are represented by white arrows and the black ones correspond to 10 m wind measured by Catalan Meteorological Service stations.